J Mol Model (2004) 10:87–93
DOI 10.1007/s00894-003-0143-z

ORIGINAL PAPER

Davor Margetić · Ronald N. Warrener · Peter W. Dibble

Diels–Alder reactivity of benzannulated isobenzofurans as assessed by density functional theory

Received: 6 February 2003 / Accepted: 5 June 2003 / Published online: 13 January 2004

Abstract Density functional theory (DFT) calculations at the B3LYP/6-31G* level for isobenzofuran **1** and eleven benzannulated derivatives of types **2** and **3** have been performed in order to compare their relative reactivities as dienes in Diels–Alder reactions. The transition state (TS) energies for their reactions with ethylene have been determined and shown to form a linear correlation between activation energies and structure count (SC) ratios. TS energies as a method for comparison of diene reactivities can be applied to IBFs bearing substituents on the ring as well as those containing heteroatoms, for which the SC ratio method failed. Different measures of aromaticity of benzannulated IBFs indicated a decrease in aromaticity going from **4** to **14**, which is also reflected in their reactivity as a dienes in Diels–Alder reaction.

Keywords Isobenzofurans · Cycloaddition · Diels–Alder reaction · Dienes · DFT calculations

Introduction

Isobenzofurans (IBFs) are a very reactive class of cyclic polyenes and enter a range of cycloaddition reactions. Their ability to act as dienes in Diels–Alder reactions has been widely exploited in synthesis, [1, 2, 3, 4, 5] some aspects of which have been conducted in our own laboratories. [6, 7, 8, 9, 10] Studies from the Wege laboratory [11] have shown that the diene reactivity of isobenzofuran can be increased by benzannulation and Dibble has recently shown that IBF **14** was the most reactive IBF yet reported. [12] Although a significant number of papers on the experimental aspects of IBFs have been published, very little has appeared on computational aspects. [13, 14, 15] The aim of this paper was to assess the ability of DFT theory to evaluate the relative reactivity in a series of benzannulated IBFs for which experimental data and a structure count (SC) correlation were available. The longer term goal is to extend this method to heterosubstituted IBFs, for which SC data are inapplicable.

D. Margetić (✉) · R. N. Warrener
Centre for Molecular Architecture,
Central Queensland University,
4701 North Rockhampton, Queensland, Australia
e-mail: margetid@emma.irb.hr

P. W. Dibble
Department of Chemistry,
University of Lethbridge,
Lethbridge, AB T1K 3M4, Canada

Computational details

All geometry optimizations and transition state calculations were performed using Gaussian98 [16] using density functional theory (DFT) with hybrid B3LYP functional (Becke's 3 parameter functional [17] with the non-local correlation provided by the expression of Lee et al. [18]) with the 6-31G* basis set on a Silicon Graphics R10000 workstation. Structures for isobenzofuran **1** and benzannulated isobenzofurans of type **2** and **3** were calculated. In order to establish their relative reactivity, transition states for their reactions with ethylene were located and activation energies estimated.

Table 1 B3LYP/6-31G* total energies (hartrees), activation energies (kJ mol^{-1}), SC ratios and heats of reactions (kJ mol^{-1})

IBF	E_{tot} GS	E_{tot} TS	E_{act}	SC ratio	ΔH_{react}
1	−383.650374	−462.213318	64.4	3	−124.7
4	−690.952856	−769.509133	82.4	2.25	−83.3
5	−767.188415	−845.744424	82.0	2.25	−81.6
6	−690.945871	−769.502004	81.6	2.33	−82.4
7	−537.303656	−615.861905	76.6	2.5	−95.8
8	−690.943322	−769.503406	71.9	2.67	−105.0
9	−690.945685	−769.505665	71.5	2.67	−105.4
10	−767.174853	−845.737470	65.3	2.67	−122.6
11	−690.933131	−769.499246	56.1	3.5	−144.8
12	−844.574881	−923.141849	53.9	3.67	−149.8
13	−537.282847	−615.851121	50.2	4	−158.6
14	−690.915473	−690.915473	43.9	5	−174.1

Results and discussion

With the exception of chryseno[2,3-c]furan **12**, all the molecules examined in this paper have been described experimentally. The reactivity for all compounds in the series has been estimated using the B3LYP/6-31G* method. Total energies, activation energies, SC ratios and heats of reaction are collected in Table 1. Dipole moments, HOMO and LUMO energy levels, atomic charges and different measures of aromaticity are shown in Table 2, while Table 3 contains different properties calculated for the transition states investigated. Figures 1

Table 2 Selected ground state parameters of IBFs **1**, **4–14** (B3LYP/6-31G*)

IBF	HOMO	LUMO	$\Delta_{(HO-LU)}$	Dipole moment	O charges	Bond alternation	C–O distance (Å)	*I*
1	–5.25	–1.13	4.12	0.41	–0.383	0.015	1.3581	60.6
4	–5.51	–1.03	4.28	0.53	–0.397	0.021	1.3615	67.3
5	–5.54	–1.25	4.29	0.47	–0.397	0.019	1.3684	67.7
6	–5.39	–1.39	4.00	0.43	–0.396	0.023	1.3622	67.9
7	–5.39	–1.07	4.32	0.48	–0.392	0.02	1.3609	65.7
8	–5.27	–1.45	3.82	0.49	–0.393	0.017	1.3578	63.8
9	–5.22	–1.39	3.83	0.44	–0.390	0.016	1.3599	63.8
10	–4.86	–1.84	3.02	0.28	–0.386	0.014	1.3581	61.3
11	–4.91	–1.74	3.17	0.21	–0.379	0.009	1.3564	60.7
12	–4.84	–1.87	2.97	0.18	–0.378	0.008	1.3558	56.1
13	–4.78	–1.84	2.94	0.20	–0.374	0.007	1.3546	54.4
14	–4.48	–2.27	2.21	0.09	–0.369	0.003	1.3528	50.5

Table 3 Selected TS parameters of **TS1**, **TS4–TS14** (B3LYP/6-31G*)

IBF	q_{CT} (e)	CC distance (Å)	HOMO (eV)	LUMO (eV)	$\Delta_{(HO-LU)}$ (eV)
1	–0.0434	2.259	–5.6	–1.47	4.7
4	–0.0385	2.2038	–5.6	–0.95	4.6
5	–0.0370	2.201	–5.4	–1.4	4
6	–0.0366	2.2042	–5.3	–1.6	3.7
7	–0.0403	2.22	–5.6	–1	4.6
8	–0.0382	2.2336	–5.6	–1.3	4.3
9	–0.0391	2.233	–5.5	–1.7	3.3
10	–0.0369	2.256	–5	–1.7	3.3
11	–0.0381	2.288	–5.2	–1.5	3.7
12	–0.0373	2.2955	–5.1	–1.7	3.4
13	–0.0392	2.3091	–5.1	–1.61	3.5
14	–0.0371	2.334	–4.7	–2.1	2.6

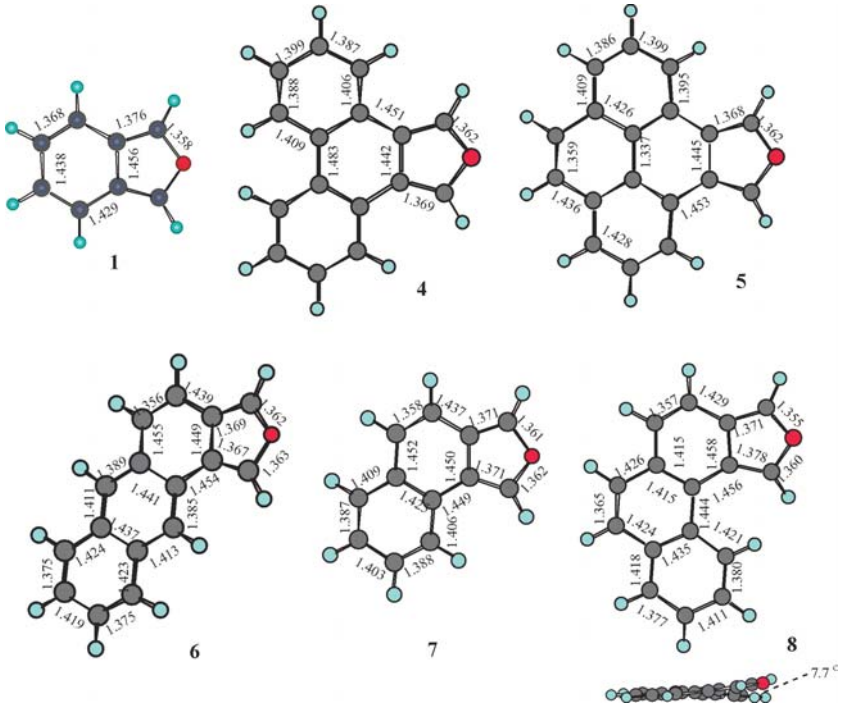

Fig. 1 B3LYP/6-31G* structures of molecules **1**, **4–8**

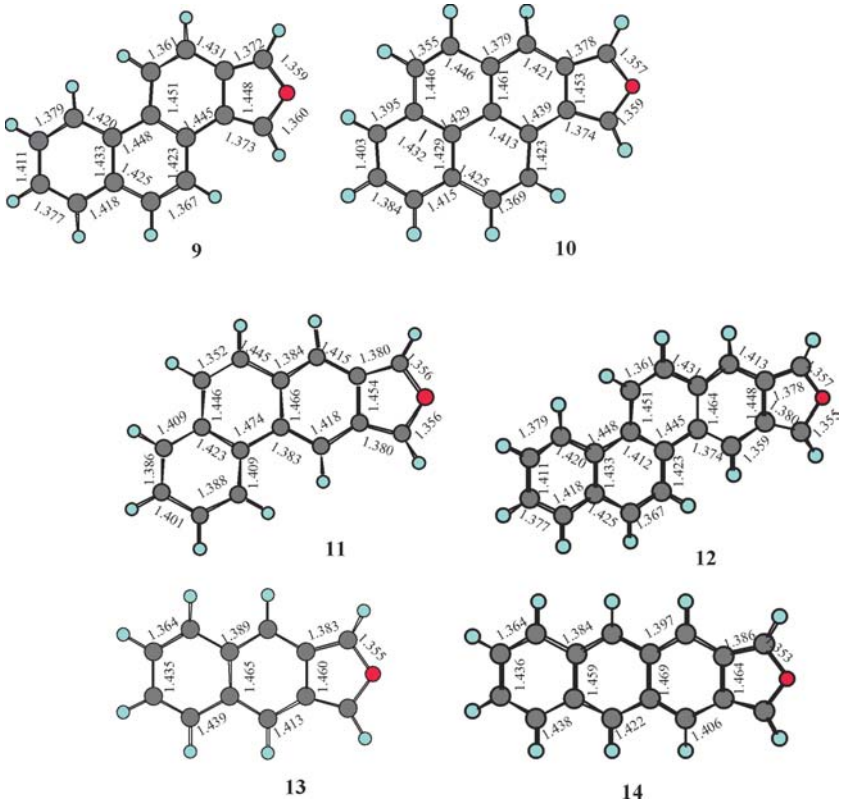

Fig. 2 B3LYP/6-31G* structures of molecules **9–14**

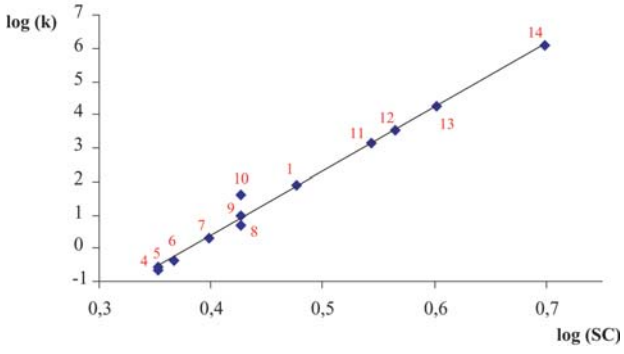

Fig. 3 Relationship between log *k* and log(SC ratio)

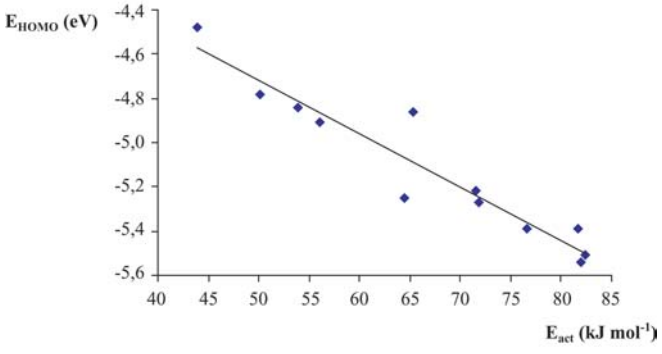

Fig. 4 Relationship between HOMO energy levels and activation energy

and 2 depict geometries of the calculated IBFs, while Fig. 3 shows the correlation between log(SC ratio) and log *k*. A correlation of activation energies with HOMO energy levels is shown in Fig. 4. Figure 5 contains bond order values for molecules **1** and **4–14**. Furthermore, Figs. 6 and 7 show calculated TS structures for the addition of IBFs **1** and **4–8** to ethylene. A correlation of activation energies with distances of newly forming carbon–carbon bonds is shown in Fig. 8. Finally, Figs. 9 and 10 show structures of TSs **9–14**.

It was suggested in the literature that the high reactivity of IBF species was a consequence of the gain in benzenoid resonance energy in going from reactants to products in the cycloaddition process. Some of this gain in resonance energy should be felt in the transition state for additions, and hence be reflected in the numerical value of rate constant. Herndon has devised a semiempirical "structure count" (SC) theory [19] which has been used by Wege to correlate the reactivities of several IBFs (towards maleic anhydride) with differences in resonance energy between reactants and products. The method was particularly simple, obtained from the numbers of classical Kekule structures that can be drawn for products and reactants. There is good correlation of SC ratios for the cycloaddition to all IBFs studied, showing a linear plot of log *k* against log(SC ratio). The gain in resonance energy was postulated to be the main contributing factor towards reactivity in the Diels–Alder reaction. The plot was later

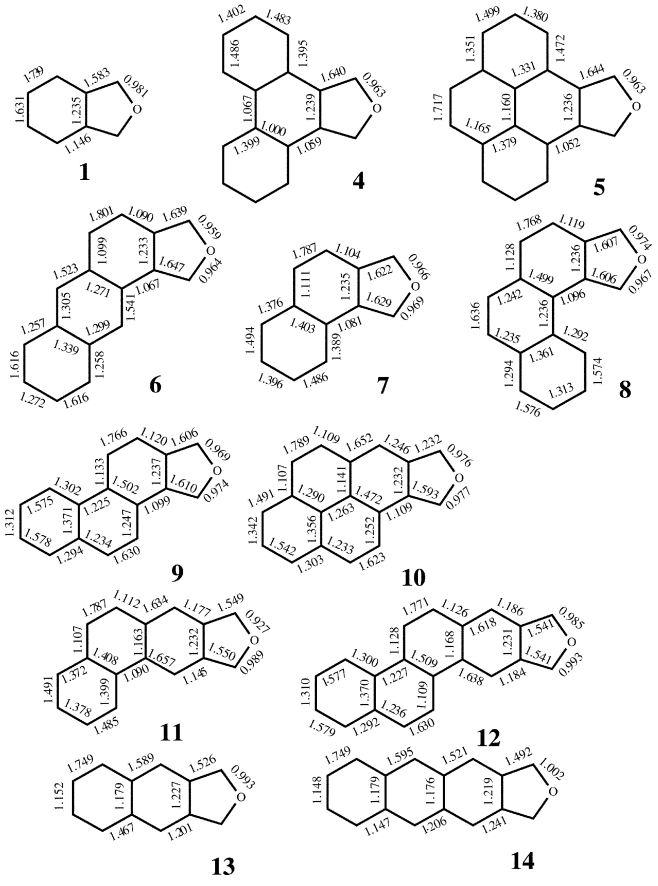

Fig. 5 Bond orders of molecules **1, 4–14**

extended by Dibble with more reactive IBFs unknown at the time Wege published his paper (Fig. 3).

Molecular structure of IBFs

To gain more insight into the reactivity of IBFs, an analysis of their ground state structures was initially conducted. The analysis of the B3LYP/6-31G* C–O interatomic distances of the IBFs studied revealed that **4** has the longest distance of 1.362 Å, while other molecules have distances in a linearly decreasing order up to molecule **14**, which has the shortest distance of 1.353 Å. For these comparisons, we have used average bond distances for all unsymmetrical IBFs (since differences in unsymmetrical molecules are small, within the range of only 0.001–0.007 Å). There was a linear correlation with the estimated activation energies, where a larger C–O bond distance corresponds to a larger activation energy. Furthermore, the analysis revealed that C–C aromatic bond distances are within a range of 1.337–1.483 Å, while single aromatic bonds are 1.389–1.483 Å, and double aromatic bonds are 1.337–1.435 Å.

Electronic structure of IBFs. HOMO–LUMO energy gap

It has been suggested that the HOMO–LUMO energy separation may serve as an index of aromaticity because a larger energy gap should increase the tendency to "retain its type", that is, to retain aromaticity by substitution, rather than addition reactions. [20, 21, 22] We found that HOMO energy levels followed a linear trend versus activation energy, where a smaller activation energy corresponded to the molecule with the highest energy HOMO value (Fig. 4). Compound **14** had the highest HOMO (–4.48 eV), while **5** had the lowest one (–5.54 eV). HOMO–LUMO energy gaps of the IBFs studied followed a similar trend, where the smallest FMO gap corresponds to IBF **14** (2.21 eV) and the largest to **5** (4.29 eV).

Aromaticity

There are numerous computational criteria of aromaticity. They can be divided into geometrical and electronic classes. [23] For instance, some of the geometrical measures include the aromaticity index (*I*), which by definition is 100 for benzene (other molecules have smaller values), bond order deviation from the average bond order [14] and bond alternation. [24] The electronic criteria include FMO gaps, [25] bond orders, and calculations [26] of magnetic properties of molecules (such as magnetic susceptibility anisotropies), [15, 27] which can be reflected in activation energies. [28] We have used some of these indices in order to evaluate the aromatic character of the IBFs studied. Our calculations showed that there was a linear correlation of activation energies against aromaticity indices (Table 2) obtained for furan rings in the series of IBFs studied. These results suggested that molecule **6** was the most aromatic (*I*=67.9) and therefore the least reactive species, while IBF **14** was the least aromatic and most reactive (*I*=50.5). Radom has used the bond-alternation parameter (or degree of delocalization) to quantify aromaticity, which was defined as the difference between the averaged single and double bond lengths in the ring. High values for the degree of bond alternation suggested a relatively high contribution of the aromatic delocalized canonical structure. When we applied this method to the furan ring of the molecules investigated, we obtained a linear correlation with activation energies, where **6** was predicted to be the most aromatic (0.023) and **14** the least aromatic (0.003), which does not fully follow the calculated activation energy trend. Furthermore, values for isotropic and anisotropic magnetic susceptibilities calculated for the furan ring showed no linear correlation with activation energies.

Dipole moments

We have also found that the dipole moments descend from molecule **4** to **14**. Compound **4** has the highest

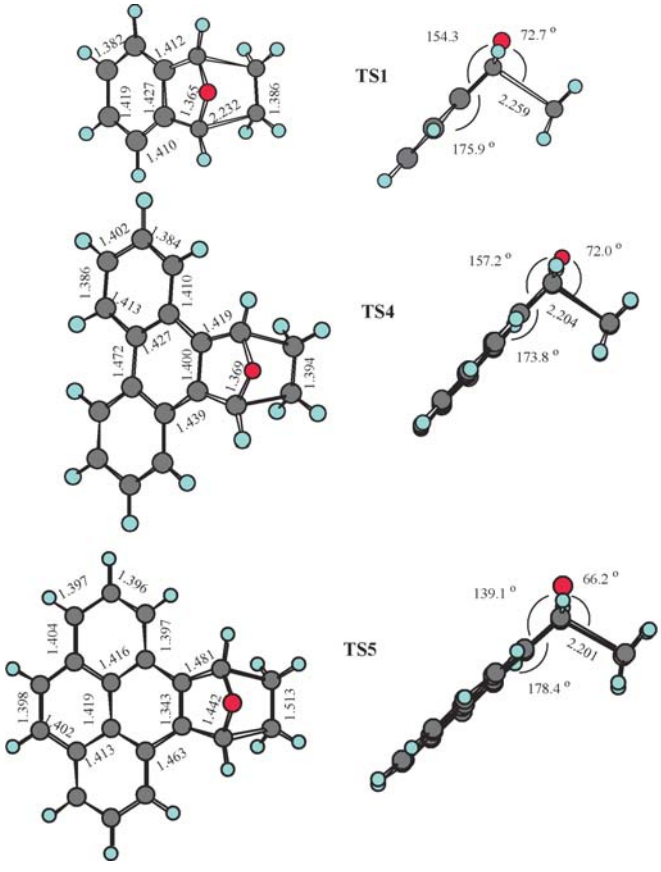

Fig. 6 B3LYP/6-31G* transition state structures **TS1**, **TS4** and **TS5**

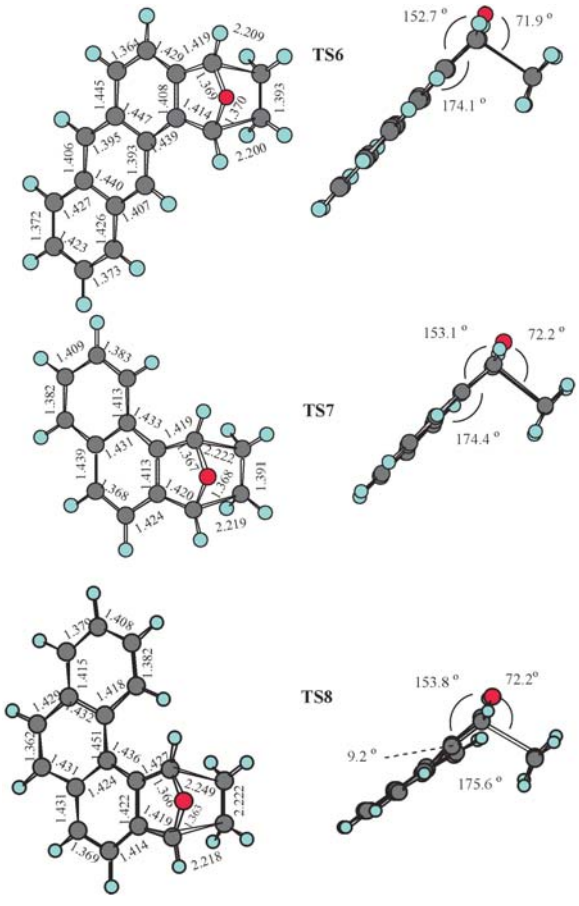

Fig. 7 B3LYP/6-31G* transition state structures **TS6–TS8**

estimated value of 0.52 Debye, while **14** has only 0.09 Debye. There is a linear relationship with the activation energy—the smallest dipole moment corresponds to the smallest activation energy. Since we computed Diels–Alder reaction of IBFs with ethylene, which was a molecule with a very small dipole moment, we believed that the reaction gained some energetic stabilization by smaller dipole–dipole repulsions in the TS. Dipole moment values are in good agreement with estimated values for atomic charges on oxygen (obtained by a Mulliken population analysis). Again, **4** had the largest value (the most negative −0.397), while IBF **14** had the smallest (−0.369). Therefore, the atomic charge on the electronegative oxygen atom contributes to the larger values of the dipole moment. However, when the same charge analysis was performed for the adjacent carbon atoms (positions 2 and 5 of the furan ring), no correlation was found. Radom has obtained similar results for atomic charges in fulvenes: at positions C1, C3 and C4 increasing charges increased the rate, but decrease for charges at C2 and C5. The correlation between the dipole moment, where an increase in dipole moment produced a decrease in rate of reaction, followed the same trend as in our calculations. [29]

Bond orders

Values for bond orders calculated for the furan ring depicted in Fig. 5 showed no linear correlation with activation energies.

Transition state structures

An analysis of transition state structures revealed that all the structures corresponded to the concerted synchronous mechanism, with values of the newly forming carbon–carbon bond distances within a range of 2.201–2.334 Å (Figs. 6, 7, 9 and 10). The degree of asynchronicity for unsymmetrical dienes was in the range of 0.003 Å (**TS9**) to 0.031 Å for **TS8**.

Figure 8 showed a correlation between the newly forming C–C bond distances and activation energies, where the TS structure that corresponded to the IBF with the highest activation energy **TS4** (82.4 kJ mol^{-1}) had the shortest C–C bond distance (2.204 Å). Similarly, the transition state structure with the smallest activation energy **TS14** (43.9 kJ mol^{-1}) has the least advanced TS with longest C–C bond distance (2.334 Å). Progress of bond formation might be a criterion for determining

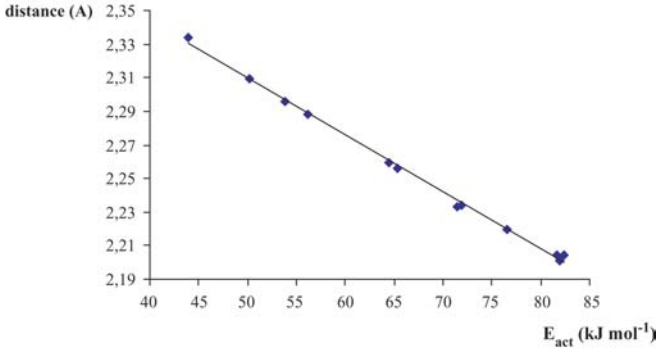

Fig. 8 Relationship between new forming C–C bond distances in TSs and activation energy

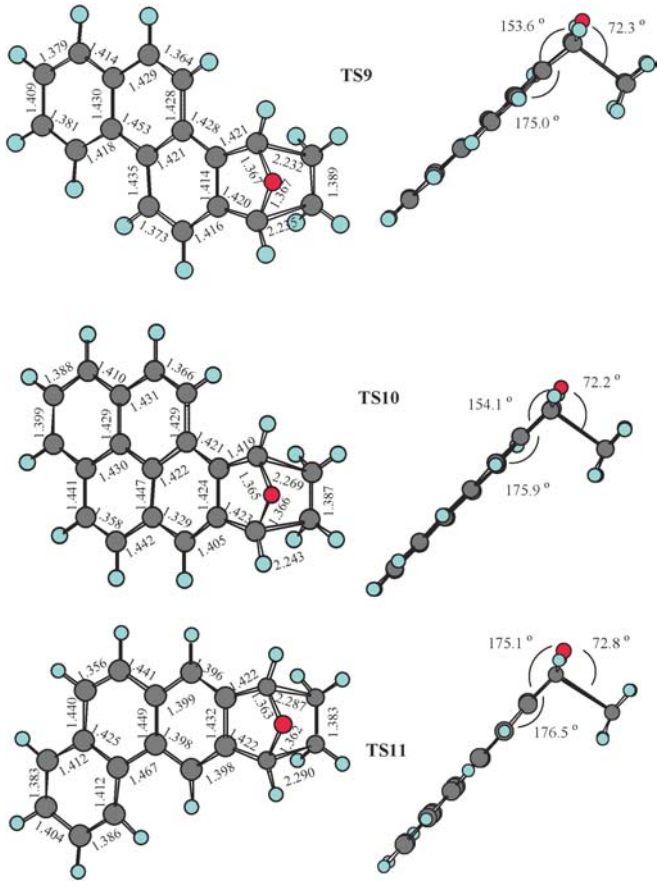

Fig. 9 B3LYP/6-31G* transition state structures **TS9–TS11**

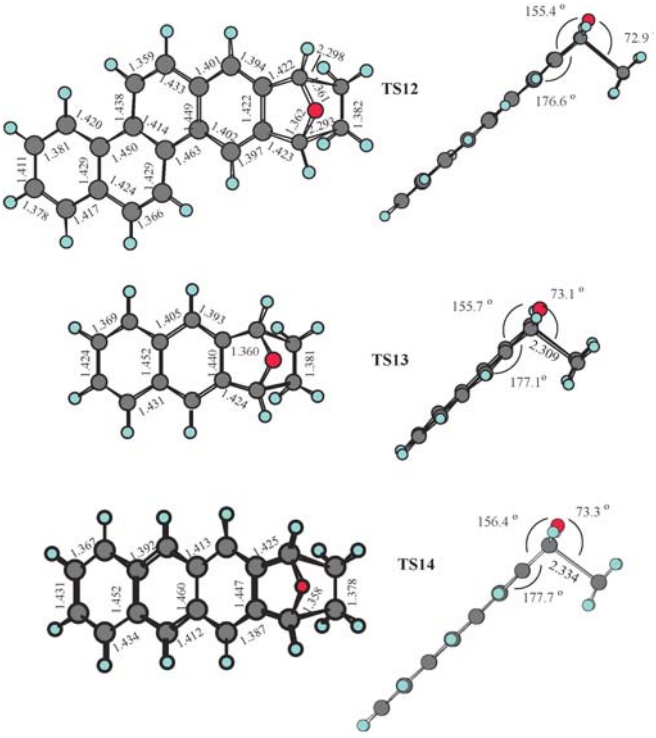

Fig. 10 B3LYP/6-31G* transition state structures **TS12–TS14**

reactivity by invoking the Hammond postulate. In very simple words, longer newly formed bonds in the transition state structure meant that the transition state structure was close in geometry to the reactants and consequently had a lower activation barrier. [30]

Furthermore, analysis of TS geometries has revealed that the dihedral angles between the $C_2O_1C_5$ plane of the furan ring and the aromatic ring plane (angle α) decreased from **TS4** (28.5°) to **TS14** (23.6°), with the exception of **TS5**. Dihedral angles between aromatic rings and the $C_2C_3C_4C_5$ plane of the furan moiety (angle β) followed the opposite trend, where **TS4** had the larger angle (173.8°) and **TS14** the smallest (177.7°), revealing the last structure as the most reactant like.

The quantum of charge transfer (q_{CT}) in the TS for all these reactions were negative (Table 3), indicating that these were normal electron-demand Diels–Alder reactions, with the electron flow from IBFs to ethylene, where IBFs acted as dienes and ethylene as a dienophile. This was previously predicted by FMO theory for the ground states of the IBFs studied. Calculated values of q_{CT} are within a range of −0.0434 (**TS1**) and −0.0366 electrons (**TS6**). Once again, we have plotted these values against activation energies and find no correlation.

Conclusion

The DFT calculations conducted at the B3LYP/6-31G* level for the range of benzannulated IBFs **1** and **4–14** have been able to provide data from which a linear relationship between Diels–Alder cycloaddition rates and structure was established. This treatment has potential application to (as yet) unknown benzannulated IBFs and in this respect corresponds with the reported ability to establish such a relationship using the simple SC method. However, the DFT method can be applied to IBFs bearing substituents on the ring as well as those containing heteroatoms. These latter features will be presented in the full paper as a separate study on hetero-atom substituted IBFs, which is currently under investigation.

Acknowledgments We thank the Australian Research Council (ARC) for funding.

References

1. Friedrichsen W (1999) Adv Heterocycl Chem 73:1–96
2. Peters O, Friedrichsen W (1995) Trends Heterocycl Chem 4:217–228
3. Wiersum UE (1981) Aldrichimica Acta 14:53–58
4. Friedrichsen W (1980) Adv Heterocycl Chem 26:135–241
5. Haddadin MJ (1978) Heterocycles 9:865–901
6. See for instance Warrener RN, Wang S, Butler DN, Russell RA (1997) Synlett 44–46
7. Warrener RN, Wang S, Russell RA, Gunter MJ (1997) Synlett 47–50
8. Warrener RN, Wang S, Butler DN, Russell RA (1997) Tetrahedron 53:3975–3990
9. Smith JG, Dibble PW, Sandborn RE (1983) J Chem Soc Chem Commun 1197–1198
10. Dibble PW, Rodrigo R (1988) Org Mass Spectrom 23:743–750
11. Moursounidis J, Wege D (1988) Aust J Chem 41:235–249
12. Tu NPW, Yip JC, Dibble PW (1996) Synthesis 77–81
13. Juršić BS (1995) J Chem Soc Perkin Trans 2 1217–1222
14. Juršić BS (1997) Tetrahedron 53:13285 –13294
15. Juršić BS (1996) J Heterocycl Chem 33:1079–1081
16. Frisch MJ, Trucks GW, Schlegel HB, Scuseria GE, Robb MA, Cheeseman JR, Zakrzewski VG, Montgomery Jr. JA, Stratmann RE, Burant JC, Dapprich S, Millam JM, Daniels AD, Kudin KN, Strain MC, Farkas O, Tomasi J, Barone V, Cossi M, Cammi R, Mennucci B, Pomelli C, Adamo C, Clifford S, Ochterski J, Petersson GA, Ayala PY, Cui Q, Morokuma K, Malick DK, Rabuck AD, Raghavachari K, Foresman JB, Cioslowski J, Ortiz JV, Stefanov BB, Liu G, Liashenko A, Piskorz P, Komaromi I, Gomperts R, Martin RL, Fox DJ, Keith T, Al-Laham MA, Peng CY, Nanayakkara A, Gonzalez C, Challacombe M, Gill PMW, Johnson B, Chen W, Wong MW, Andres JL, Gonzalez C, Head-Gordon M, Replogle ES, Pople JA (1998) Gaussian 98, Revision A.5. Gaussian, Pittsburgh, Pa.
17. Becke AD (1993) J Chem Phys 98:1372–1377
18. Lee C, Yang W, Parr RG (1988) Phys Rev B 37:785–789
19. Herndon WC (1975) J Org Chem 40:3583–3586
20. Pearson RG (1989) J Org Chem 54:1432–1435
21. Zhou Z, Parr RG (1989) J Am Chem Soc 111:7371–7379
22. Bean GP (1998) J Org Chem 63:2497–2506
23. Katritzky AR, Barczynski P, Musumarra G, Pisano D, Szafran M (1989) J Am Chem Soc 111:7–15
24. Scott AP, Agranat I, Biedermann PU, Riggs NV, Radom L (1997) J Org Chem 62:2026–2038
25. Juršić BS (1999) Theochem 468:171–179
26. Manoharan M, De Proft F, Geerlings P (2000) J Chem Soc Perkin 2 8:1767–1773
27. Subramanian G, Schleyer PvR, Jiao H (1996) Angew Chem, Int Ed Engl 35:2638–2641
28. Juršić BS (1998) Theochem 427:165–169
29. Gugelchuk MM, Chan PCM, Sprules TJ (1994) J Org Chem 59:7723–7731
30. Hammond GS (1955) J Am Chem Soc 77:334–338